# Self-calibration of Laser Tracking Systems

Hanqi Zhuang*, Shui H. Motaghedi**, Zvi S. Roth*, and Ying Bai*

*Department of Electrical Engineering
Florida Atlantic University
Boca Raton, FL 33431

** Jet Propulsion Laboratory
California Institute of Technology
4800 Oak Grove Drive
Pasadena, California 91109

**Abstract**

In this paper, a methodology for self-calibrating a multi-beam laser tracking measurement system with planar constraints is proposed. A model for the multiple-beam laser tracking system is derived. Through error analysis it is shown that using even rough angular measurement of the gimbal joint positions may improve the overall system calibration results. Parameter observability issues are studied for self-calibrating the multiple-beam laser tracking system. The results reveal the applicability of planar constraints to the system self-calibration. Results of simulation and experimentation on a prototype system are reported to show the applicability of the proposed calibration strategies.

## 1. Introduction

Laser tracking systems have advanced rapidly since 1980's because of a growing worldwide effort to develop internationally accepted procedures and terminology for the measurement and description of robot performance [1 ].

Lau and his colleagues from National Bureau of Standards [1 ] were among the first to develop a laser tracking system for rapid measurement of the positional accuracy of robots. The laser tracking system Lau produced was an automatic, spherical coordinate laser measurement system, where a laser interferometer is accurately pointed, by means of a two-angle servo system, to a reflector attached to the robot wrist. A further refinement 5-D Laser tracking system was soon proposed by Lau et al [2 ] that could determine the three dimensional static and dynamic positional accuracy of a robot end-effector to a few parts in 100,000, and wrist orientations to within 2 arc seconds.

Mooring [7] proposed a model that features several geometric error parameters to account for the gimbal rotation axes which are neither orthogonal and nor intersecting. His rather interesting calibration strategy employed a grid of target points (refer to Figure 1) placed at a location that allows the reflected beam to strike any of the grid points. The target points are on a planar surface and the location of each point is precisely known in the target coordinate system. The calibration problem is then reduced to that of finding a set of parameters in the system so that the difference between the computed target location and the actual target location is minimized.

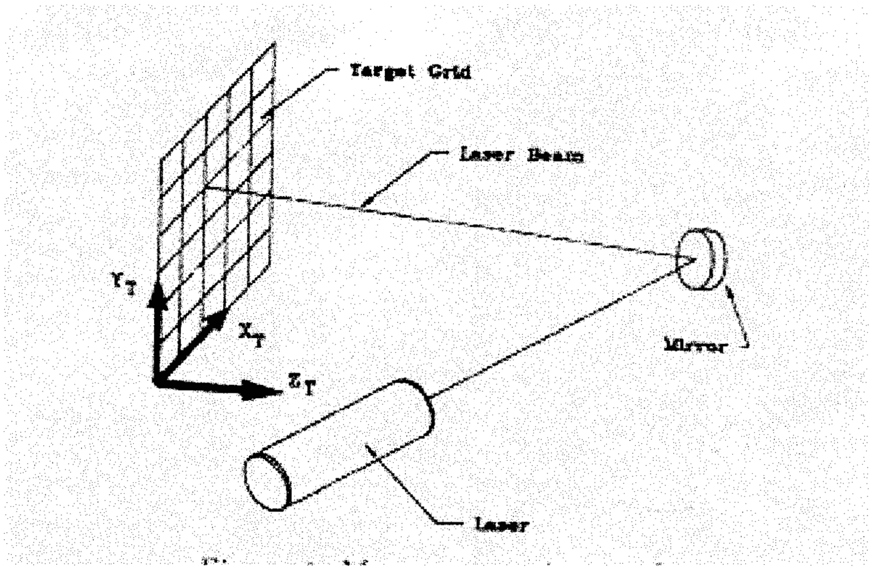


Figure 1 Mooring's Calibration Strategy proposed

Parker et al [8] from National Radio Astronomy Observatory have used a rangefinder (Figure 2) with the fast multiple range capability to carry out two tasks: (1) measurement of the shape of a reflector surface and correction for changes due to gravity and thermal effects. (2) relating the positions of all the measured surface points to a reference frame of points fixed in the ground around the telescope. The rangefinder uses the propagation time of a beam of infrared radiation to measure distances of up to 120 m with errors of less than 50 $\mu$m.

Greenleaf [9] introduced the multi-lateration method into the 3-D laser tracking measuring. He used a four single-beam laser tracking interferometers and a common cat's eye target to obtain μm precision measurements. Three length measurements of a single target provided by three trackers uniquely determine the location of the target point in 3-D space. The fourth laser tracker incurs a redundancy in the data so the instrument parameters such as the interferometer counter offsets can be estimated numerically from a number of position reading.

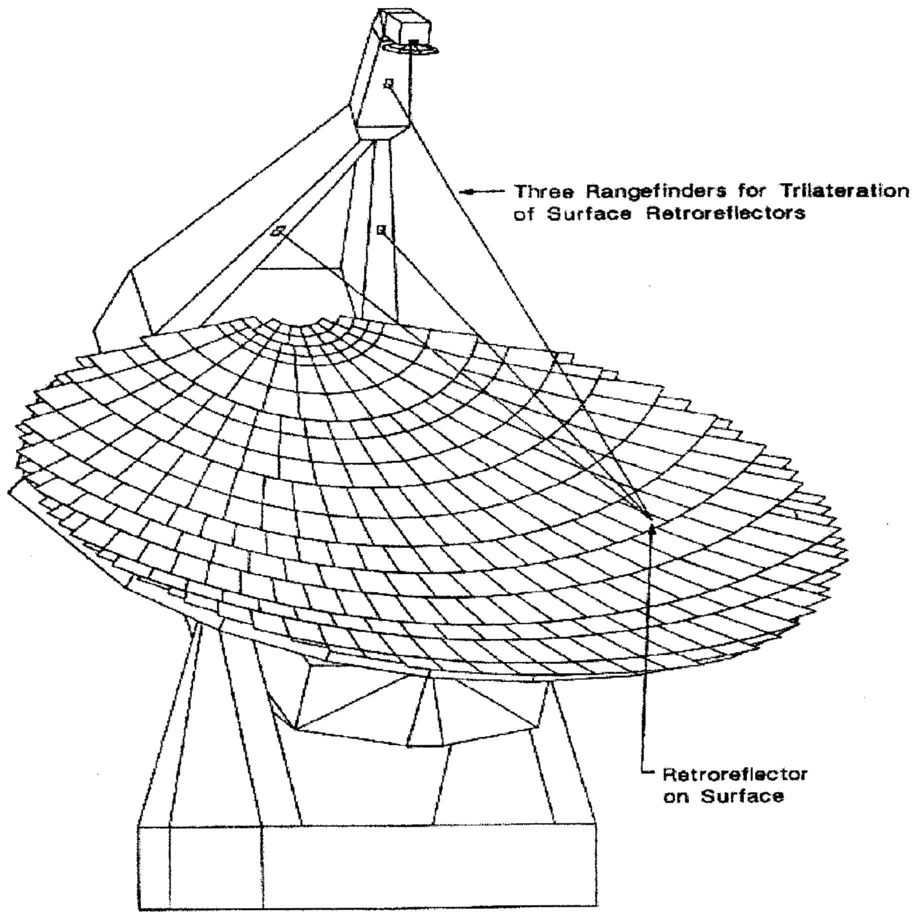


Fig. 1. The geometry of the metrology system.

Figure 2 Geometry of the metrology system developed by NRAO

Zhuang and Roth [4 ][5 ] too used multi-lateration method for the self-calibration of a multiple-beam laser tracking system. Four trackers follow a common retroreflector attached a moving target. Each tracker has a tracking mirror mounted on two orthogonal rotation axes. The mirrors are rotated based on the offset position of the retro-reflected beam in order to aim the laser beam at the target center. The three length measurements combined with the knowledge of the three mirror center location provide a means to compute the target positions. A least-squares technique is used to calibrate all the parameters in the overdetermined system. Zhuang and Roth [6 ] later proposed a model to include all these geometric errors which satisfies the model requirements of completeness, proportionality, and equivalence [12].

In this paper, a methodology for self-calibrating the laser tracking measurement system was proposed. A model characterizes the multiple-beam laser tracker system was derived. Through error analysis it is shown that even rough angular measurement may improve the overall system calibration results. Various calibration strategies utilizing planar constraints were proposed to deal with different system setups. For each calibration strategy, observability issues on estimating unknown parameters were studied. The results revealed the applicability of the planar constraints to the system self-calibration. Results from simulations and experimental studies are reported.

## 2. Modeling of a Multiple-Beam Laser Tracking System

A multiple-beam laser tracking system needs to have a minimum of three trackers for the calculation of target positions. The kinematic relationship among the three trackers is depicted in Figure 3. Let the base coordinate system of tracker 1 serve as the reference coordinate system of the entire multi-beam laser tracking system. The transformation from the base coordinate of tracker $k$ to that of tracker $j$ is denoted by ${}^{j}\boldsymbol{T}_k$ , for $j$, $k$ = 1, 2, 3, the distance from the beam point of incidence on the mirror of the $k$th tracker to the target is denoted by $l_k$. Let the target position with respect to the reference coordinate system be denoted by $\boldsymbol{r}$. Let the point of incidence at the mirror surface of the $k$th tracker be denoted by $\boldsymbol{c}_k$ . Point $\boldsymbol{c}_k$ is represented with respect to the $k$th tracker base coordinate system. These are assumed known for the time being. Let us also assume that ${}^{1}\boldsymbol{T}_2$ , ${}^{1}\boldsymbol{T}_3$ , and $l_k$ for $k$ = 1, 2, 3 are known. These assumptions characterize a well-calibrated system. One is then able to compute the target position in the reference coordinate system.

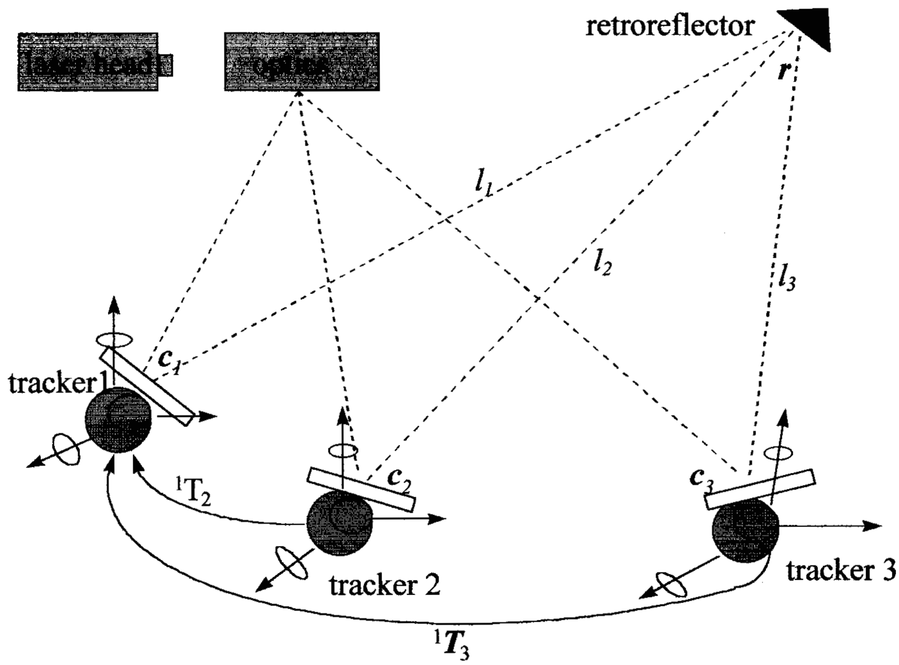


Figure 3 Schematic of a multiple-beam laser tracking system

Whenever a gimbal's angular measurements as well as the distance measurements of the laser interferometers are used, one is able to compute the target position, provided that each tracker is tracking a distinct target point on the moving rigid object. The orientation of the target can also be measured if each tracker is locked on a different retroreflector. However, angular measurements of a gimbal are typically inferior to the distance measurements of a laser interferometer in terms of resolution. The following sections discuss the computation of target positions using distance measurements only as well as joint angular and distance measurements.

## 2.1 Target position computation using distance measurement only

For coordinate measuring that is based on distance measurements only, a minimum number of three trackers are needed. It is assumed for the time being that there is neither mirror center offset nor gimbal axis misalignment. The target coordinates are obtained from the distance measurements by triangulation based on the knowledge of the locations of the three trackers ( i.e., the relative distances among the mirror centers ) and a reference point in the world coordinate frame.

Using only distance measurements in computing the coordinate measurements can be accurate only when the laser tracking system is ideal. If the mirror centers shift while the trackers are following the target, angular measurements need to be included in the model to avoid large errors. Angular measurements, although being relatively inaccurate, are useful in predicting the mirror center locations, which are in turn used to compute the target position along with the distance measurements. In the next section both distance and angular measurements are used to calculate the target measurements.

## 2.2 Target position computation using both angular and distance measurements

The setup of the multiple-beam system is as shown in Figure 4. Let the base coordinate system of tracker 1 be the reference coordinate system of the multi-beam laser tracking system. Frames $\{1\}$, $\{2\}$ and $\{3\}$ are the local frames of the three trackers respectively. The nominal mirror center of trackers 1, 2 and 3 are at the origins of frames $\{1\}$, $\{2\}$ and $\{3\}$. The transformation from the base coordinate of tracker $k$ to that of tracker $j$ is denoted by ${}^{j}\boldsymbol{T}_{k}$, for $j$, $k = 1, 2, 3$. The distance from the $kth$ mirror center to the target is denoted by $l_k$. Let $A$, $B$ and $C$ represent the points of actual beam incidence at the mirror surface of the $k$th ( $k = 1, 2, 3$ ) tracker. The axes of frame $\{A\}$ are parallel to those of $\{1\}$, $\{2\}$ and $\{3\}$. Their origins are at point $A$, $B$ and $C$ respectively. A coordinate frame $\left\{A'\right\}$ is placed so that its origin is at point $A$, its $x$ axis is coincident with line $AB$, and its $x$-$y$ plane contains lines $AB$ and $AC$. Frame $\left\{A'\right\}$ is placed so that the coordinates of the target are simple with respect to this coordinate system.

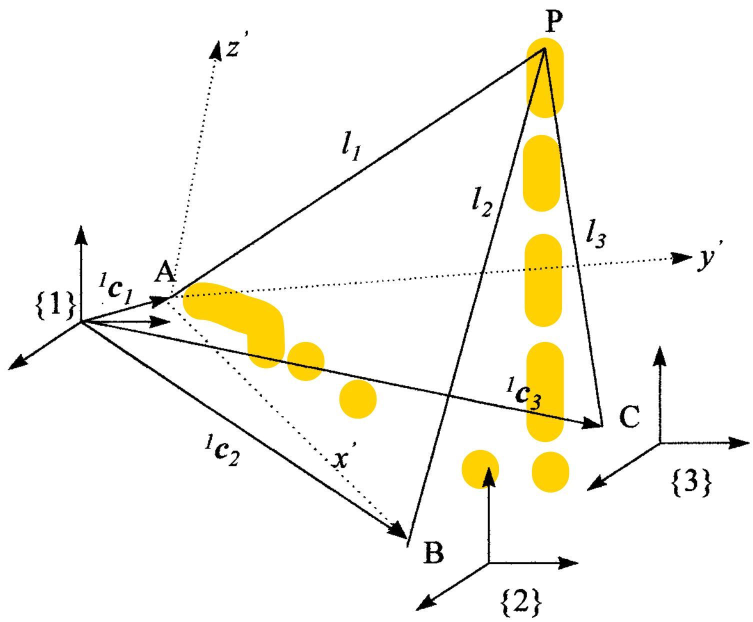


Figure 4 The system set of multiple-beam laser tracker

Let the coordinates of the beam incidence point on the mirror surface of the $k$th ($k$ = 1, 2, 3) tracker be $c_k$ in their respective coordinate frame. Note that $c_k$ is a function of the 10 parameters of the respective single-beam laser tracker as well as the tracker's gimbal angles. Whenever the gimbal moves, $c_k$ also changes. Given the 10-parameter single-beam tracker model derived in [6], along with the gimbal angular distance measurement, $c_k$ can be computed. $c_k$ may then be transformed to the reference coordinate frame by ${}^1\boldsymbol{T}_k$. Let the (3x3) rotation submatrix and (3x1) position vector of ${}^1\boldsymbol{T}_k$ be ${}^1\boldsymbol{R}_k$ and ${}^1\boldsymbol{t}_k$, respectively. Then,

$$ {}^1\boldsymbol{c}_k = {}^1\boldsymbol{R}_k \boldsymbol{c}_k + {}^1\boldsymbol{t}_k \qquad \text{for } k=1, 2, 3 \qquad (1) $$

The target position $\boldsymbol{r}$ is therefore an intersection point of three spheres centered at ${}^1\boldsymbol{c}_k$ with radius $l_k$ each. The intersection point is not unique, however the target position can always be practically determined by the physical configuration of the LTS. The following elements are considered known for the computation of the target position with regard to the reference frame {1}.

1) $c_1$, the coordinates of $A$, is known with respect to $\{1\}$ by the first tracker model.

$c_2$, the coordinates of $B$, is known with respect to $\{2\}$ by the second tracker model.

$c_3$, the coordinates of $C$, is known with respect to $\{3\}$ by the third tracker model.

2) ${}^1T_2$, the transformation matrix from $\{2\}$ to $\{1\}$, is known.

${}^1T_3$, the transformation matrix from $\{3\}$ to $\{1\}$, is known.

3) $l_1$ , $l_2$, $l_3$ the distances from $A$, $B$, $C$ to $P$ are known. ( $l_1$ , $l_2$ , $l_3$ are compensated using $l_{s,i}$ $(\rho_k$ , $\theta_k)$ [10]), where $(\rho_k$ is the kinematic parameter vector and $\theta_k$ is the joint variable vector of the $k$th gimbal.

In the remaining part of this section, a set of equations is derived for computing the target position in the reference frame $\{1\}$. Note that all the single-beam tracker models and the transformations among the trackers are assumed pre-calibrated for the target position computation. The key step is to transform the vectors $c_k$ from their respective tracker coordinate frames to the reference coordinate frame through the transformation matrices among the trackers. To be able to use the results for computing the target position given in [4], $A$, $B$ and $C$ the points of the beam incidence, are needed to be transformed to the frame $\{A'\}$. The target point $P$ is then computed in frame $\{A'\}$. Finally, the position vector is transformed from $\{A'\}$ to $\{1\}$ through a sequence of transformations.

Step 1. The transformation matrix relating $\{A\}$ to $\{1\}$ is ${}^1T_A = \begin{bmatrix} I & c_1 \\ 0 & 1 \end{bmatrix}$,

The transformation matrix relating $\{B\}$ to $\{2\}$ is ${}^1T_B = \begin{bmatrix} I & c_2 \\ 0 & 1 \end{bmatrix}$,

The transformation matrix relating $\{C\}$ to $\{3\}$ is ${}^1T_C = \begin{bmatrix} I & c_3 \\ 0 & 1 \end{bmatrix}$.

Step 2. Represent $c_2$, $c_3$ in $\{A\}$, which are denoted by ${}^A c_2$, ${}^A c_3$. For instance,

$${}^A c_2 = {}^A T_2 c_2 = {}^A T_1 {}^1 T_2 c_2 \qquad \text{and} \qquad {}^A c_3 = {}^A T_3 c_3 = {}^A T_1 {}^1 T_3 c_3$$

Step 3. Represent $c_2$, $c_3$ in $\{A'\}$. Denote ${}^{A'}R_A = \{x^T, y^T, z^T\}$, where

$$x^T = \begin{pmatrix} \|{}^A c_2\| \\ 0 \\ 0 \end{pmatrix} \qquad z^T = \frac{{}^A c_2 \times {}^A c_3}{\|{}^A c_2 \times {}^A c_3\|} \qquad y^T = z^T \times x^T$$

Thus, the position of *B* with regard to $\{A'\}$ is: ${}^{A'} c_2 = {}^{A'} R_A {}^A c_2$ and

The position of *C* with regard to $\{A'\}$ is: ${}^{A'} c_3 = {}^{A'} R_A {}^A c_3$

The coordinates of *B* and *C* with regard to $\{A'\}$ are now derived. By following the same triangulation process as in Section 2.1, the target position in $\{A'\}$ can be calculated through the knowledge of the coordinates of *B*, *C* and the three distances $l_1$ , $l_2$, $l_3$. The coordinates of the target *P* with respect to $\{A'\}$ is (refer to Figure 4) [4],

$$r_x = \frac{l_1^2 - l_2^2 + {}^{A'}c_{2,x}^2}{2 \cdot {}^{A'}c_{2,x}} \tag{2}$$

$$r_y = \frac{l_1^2 - l_3^2 + {}^{A'}\mathbf{c}_3 \cdot {}^{A'}\mathbf{c}_3 - 2 r_x \cdot {}^{A'}c_{3,x}}{2 \cdot {}^{A'}c_{3,y}} \tag{3}$$

$$r_z = \pm\sqrt{l_1^2 - r_x^2 - r_y^2} \tag{4}$$

where $r_x$, $r_y$ and $r_z$ are the x, y, and z coordinates of the target point in the reference frame.

The target position with respect to frame $\{1\}$ is

$${}^1 r = {}^1 T_A {}^A T_{A'} r \tag{5}$$

where ${}^{A}\boldsymbol{T}_{A'} = \begin{bmatrix} {}^{A}\boldsymbol{R}_{A'} & 0 \\ 0 & 1 \end{bmatrix}$.

## 2.3 Sensitivity analysis of the multiple-beam system

The argument is that even though the angular measurement accuracy of a gimbal is inferior to that of the distance measurement in a laser interferometer, the angular measurement may still be used to predict the coordinates of the beam incidence point at the mirror surface of the each tracker. This claim will be backed by both sensitivity analysis and numerical simulations. A differential transformation, which relates the parameter errors to the measurement residuals plays an important role in the sensitivity analysis. The differential transformation corresponding to the kinematic model of the laser tracking system presented in Section 2.2 is derived next.

Let us consider the kinematic model of laser tracking system. The variables $\boldsymbol{r}$ and ${}^{r}\boldsymbol{c}_k$ ($k$=1, 2, 3) are represented in the reference coordinate system. The target position satisfies the following equation,

$$({}^{1}\boldsymbol{r} - {}^{1}\boldsymbol{c}_k)\cdot({}^{1}\boldsymbol{r} - {}^{1}\boldsymbol{c}_k) = \boldsymbol{l}_k^2, \qquad \boldsymbol{k} = 1,2,3 \tag{6}$$

where ${}^{1}\boldsymbol{r}$ and ${}^{1}\boldsymbol{c}_k$ ( $k$=1, 2, 3 ) are coordinates of the target and the beam incidence on the $k$th mirror represented in coordinate system {1}. Perturbing both sides of equation ( 6 ) yields,

$$({}^{1}\boldsymbol{r} - {}^{1}\boldsymbol{c}_k)^T (d\,{}^{1}\boldsymbol{r} - d\,{}^{1}\boldsymbol{c}_k) = l_k dl_k, \qquad k = 1,2,3 \tag{7}$$

or,

$$({}^{1}\boldsymbol{r} - {}^{1}\boldsymbol{c}_k)^T d\,{}^{1}\boldsymbol{r} = ({}^{1}\boldsymbol{r} - {}^{1}\boldsymbol{c}_k)^T d\,{}^{1}\boldsymbol{c}_k - l_k dl_k \quad k=1,2,3 \tag{8}$$

Identification of $d\,{}^{1}\boldsymbol{c}_k$ and $dl_k$ enables of effective compensation of $d^{1}\boldsymbol{r}$. In order to study $d\,{}^{1}\boldsymbol{c}_k$, let $d\boldsymbol{c}_k$ be analyzed first. The error $d\,{}^{1}\boldsymbol{c}_k$ is then related to $d\boldsymbol{c}_k$ by a fixed transformation.

For the one-tracker configuration, there is a formula relating $l_m$ , $l_s$ and $l_r$ to $l$ which is described in [6],

$$l_m + l_r = l + l_s \tag{9}$$

The notation is defined following equation ( 10 ). As three trackers are used in the system, the tracker index $k$ is introduced,

$$l_k = l_{m,k} + l_{r,k} - l_{s,k} \qquad k=1,2,3 \tag{10}$$

where $l_k$ is the distance from the point at which the incident beam hits the mirror surface on the $kth$ tracker to the target location, $l_{m,k}$ is the relative distance measured by the $k$th tracker, $l_{r,k}$ is the distance from the reference point to the $kth$ tracker. $l_{s,k}$ is the distance from the point at which the incident beam hits the mirror surface on the $kth$ tracker corresponding to the reference point to the point at which the incident beam hits the mirror surface on the $k$th tracker corresponding the target location [6]. Perturbing ( 10 ),

$$dl_k = dl_{m,k} + dl_{r,k} - dl_{s,k} \qquad k=1,2,3 \tag{11}$$

Normally, the measurement accuracy of the beam travel distance is much better than that of the tracker gimbal angles. Therefore $dl_{m,k}$ can be neglected. The remaining terms are

$$dl_k = dl_{r,k} - dl_{s,k} \tag{12}$$

The beam incidence $\boldsymbol{c}$ on the mirror with regard to the local tracker coordinate system is:

$$\boldsymbol{c} = \boldsymbol{c}_r + l_s \boldsymbol{b}_I \tag{13}$$

where $\boldsymbol{c}_r$ is the coordinates of the point at which the incident beam hits on the mirror surface on the tracker corresponding to the reference point. $\boldsymbol{b}_i$ is the incoming beam direction with respect to the tracker coordinate system.

Using the tracker index, we write

$$\boldsymbol{c}_k = \boldsymbol{c}_{r,k} + l_{s,k}\boldsymbol{b}_{I,k} \qquad k=1,2,3 \qquad (14)$$

Perturbing ( 14 ) yields

$$d\mathbf{c}_k = d\mathbf{c}_{r,k} + \boldsymbol{b}_I dl_{s,k} + l_{s,k} d\boldsymbol{b}_{I,k} \qquad k=1,2,3 \qquad (15)$$

In ( 12 ) and ( 15 ), $dl_{r,k}$, $d\boldsymbol{b}_I$ and $dc_{r,k}$ are fixed errors as these are functions of fixed parameters. It is assumed that these fixed errors can be compensated through calibration. In other words, the effect of angular measurement noise on the measurement accuracy of target point is of main interest. These errors are reflected in $dl_{s,k}$. $dl_{s,k}$ is a function of the *kth* gimbal joint angles $\theta_{1,k}$ and $\theta_{2,k}$. Some lengthy derivation can establish that $dl_{s,k}$ is indeed negligible [10].

In summary, the main objective of calibrating each tracker is to obtain kinematic error parameters of these trackers that can be used along with angular measurements, to predict the beam length adjustment $l_{s,k}$ and the incident point $\boldsymbol{c}_k$ (the subscript $k$ is the tracker index). Since the angular measurements of the gimbals are not sufficiently accurate, the predicted incident point is further compensated by $dc_k$.and the length measurement $l_k$ is modified by $dl_k$. Let $l_{r,k}^0$ be the laser beam length offset provided by the calibration of each individual tracker, $c_k^0$ represents the beam incidence on the $k$th tracker mirror provided by the calibration. The mirror center offset $\boldsymbol{c}_k$ and the beam length offset can then be computed by the following equations:

$$\boldsymbol{c}_k = \boldsymbol{c}_k^0(\rho_k, \theta_k, l_k) + d\boldsymbol{c}_k \qquad (16)$$

$$l_k = l_{m,k} + l_{r,k}^0 + dl_k - l_{s,k}(\rho_k, \theta_k) \qquad (17)$$

where $\rho_k$ and $\boldsymbol{\theta}_k = [\theta_{1,k} \quad \theta_{2,k}]^T$ are respectively the parameter and joint vectors of the $k$th tracker. It is essential representing $\boldsymbol{c}_k^0$ and $l_{i,k}^0$ in terms of tracker joint and parameter vectors. Substituting ( 16 ) into (1) yields

$$ {}^1\boldsymbol{c}_k = {}^1\boldsymbol{R}_k(\boldsymbol{c}_k^0 + \boldsymbol{dc}_k) + {}^1\boldsymbol{t}_k \tag{18} $$

$\boldsymbol{dc}_k$ and ${}^1\boldsymbol{t}_k$ cannot be separately identified since ${}^1\boldsymbol{R}_k$ is fixed. Fortunately for the purpose of compensation, these do not need to be separately computed. The errors represented by $\boldsymbol{dc}_k$ can be absorbed by ${}^1\boldsymbol{t}_k$. Therefore, ( 18 ) becomes

$$ {}^1\boldsymbol{c}_k = {}^1\boldsymbol{R}_k\boldsymbol{c}_k^0 + {}^1\boldsymbol{t}_k = {}^1\boldsymbol{R}_k\boldsymbol{c}_k^0(\rho_k, \theta_{1,k}, \theta_{2,k}, l_k) + {}^1\boldsymbol{t}_k \tag{19} $$

where $\boldsymbol{c}_k^0$ is the beam incidence on the $k$th tracker mirror which can be predicted using ( 14 ) and ${}^1\boldsymbol{t}_k$ can be calibrated. $\boldsymbol{c}_k^0$ is the beam incidence on the *kth* tracker mirror provided by the calibration of individual trackers. Since the gimbal angles $\theta_{1,k}$ and $\theta_{2,k}$ are inferior to the distance measurements, $\boldsymbol{c}_k^0$ does not accurately represent the beam incidence. However, the error caused by the inaccuracy of the gimbal angles measurements can be compensated by the translation vector ${}^1\boldsymbol{t}_k$ during the calibration procedures. Therefore, ${}^1c_k$ on the left hand side of ( 19 ) accurately represents the beam incidence on the $k$th tracker with regard to the coordinate system {1}. Following the calculation of the beam incidences of each individual tracker, the target coordinates can be computed by Equation ( 2 ) through ( 4 ).

## 3. Observability issues

This section explores the parameter observability of the calibrated multiple-beam laser tracking system; refer to Figure 5.

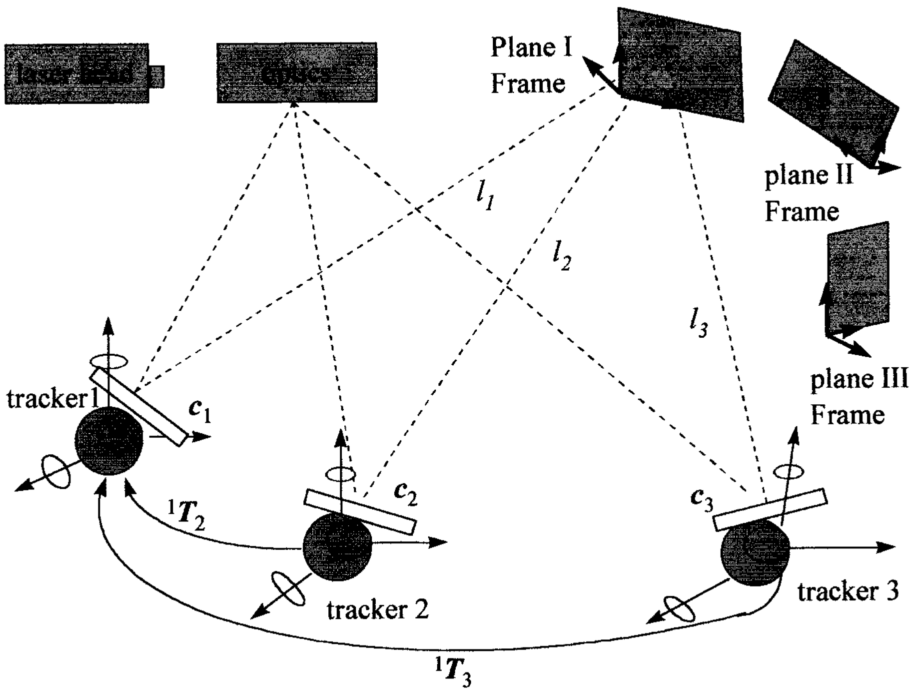


Figure 5 Calibration scheme of a multiple-beam laser tracking CMM

The three-beam laser tracking CMM involves real-time measurements of the tracker gimbal angles and the (interferometric) relative distance from the laser tracker to the points on the planes. The number of points to be measured on each plane should exceed the total number of parameters to be calibrated, as each measurement only generates one measurement equation. In the calibration process, either one of the coordinate systems in the planes or the machine base coordinate system may be chosen as the reference frame for the whole system.

Two calibration strategies are proposed next. In the first, one of the plane is used to define a reference coordinate system, and the plane parameters are treated as known. The entire system is calibrated in two stages. In the first stage, the transformation from the reference system to the base system of each tracker is identified, together with the parameters of each tracker. In the second stage, we calibrate the two of the transformations that relate the three trackers to each other, as well as the beam length offsets in each tracker. Note that the transformations among the three trackers can be extracted from the model obtained in the first stage. However, recomputing of these transformations in the second stage improves the calibration accuracy.

In the second method, the plane parameters are considered unknown. The reference coordinate system is defined by the base coordinate system of the first tracker. The individual laser trackers are calibrated first. By doing so, the unknown geometric parameters of each laser tracker, together with the plane parameters, are estimated. The second stage of this method is identical to that of the first method. The two calibration methods are explained in more detail next.

A major task of calibrating a multiple-beam laser tracking system is to identify the relative transformation between each pair of individual trackers. Let the (3×3) rotation submatrix and (3×1) position vector of ${}^1\boldsymbol{T}_k$ be ${}^1\boldsymbol{R}_k$ and ${}^1\boldsymbol{t}_k$ respectively. Then,

$$ {}^1\boldsymbol{c}_{k,,i} = {}^1\boldsymbol{R}_k \boldsymbol{c}_{k,i} + {}^1\boldsymbol{t}_k \text{ for } k = 1, 2, 3 \qquad (20) $$

where $\boldsymbol{c}_k$ ( $k$=1, 2, 3 ) is the mirror center offset at the $k$th tracker local coordinate frame and ${}^1\boldsymbol{c}_k$ is the $k$th mirror center offset with regard to the reference coordinate frame. The governing equations for computing target point $\boldsymbol{r}$ using distance measurements are

$$ ({}^1\boldsymbol{R}_k \boldsymbol{c}_{k,i} + {}^1\boldsymbol{t}_k - \boldsymbol{r})^T ({}^1\boldsymbol{R}_k \boldsymbol{c}_{k,i} + {}^1\boldsymbol{t}_k - \boldsymbol{r}) = l_k^2 \quad \text{for } k = 1, 2, 3 \qquad (21) $$

where ${}^1\boldsymbol{R}_k$ and ${}^1\boldsymbol{t}_k$ are respectively the rotation submatrix and position vector of ${}^1\boldsymbol{T}_k$ , and ${}^1\boldsymbol{T}_1$ is a 4x4 identity matrix. Since each individual gimbal has been pre-calibrated, $\boldsymbol{c}_{k,i}$ and $l_k$ can be computed with the measured gimbal angles and distances.

In [10], it is shown that whemever planar constraints are used to calibrate a robotic system, a necessary condition is that the kinematic parameters of the unconstrained system are observable. The next section examines the observability of the unconstrained system for two related cases.

### 3.1 Case 1: gimbal angular measurements relatively accurate

Whenever the angular measurements of all the trackers are relatively accurate, the only unknowns are transformations ${}^1\boldsymbol{T}_2$ and ${}^1\boldsymbol{T}_3$ . These transformations can be determined if target points are computed independently by each tracker. This problem is equivalent to the problem of determining a transformation that maps a set of points from one coodinate frame to another, and solutions can be found in [11].

One may also use an iterative procedure to further improve the accuracy of estimation. In this case, an error model that relates the measurement vector to the parameter error vector is essential in studying the observability of the system. To this end, the error model is derived next.

In ( 21 ), ${}^1\boldsymbol{R}_k$, ${}^1\boldsymbol{t}_k$, and $\boldsymbol{r}$ are variables to be adjusted iteratively. $\boldsymbol{c}_{k,i}$ and $l_k$ can be computed with measured gimbal angles, distances and the parameters which are pre-calibrated in each individual laser tracker. Perturbing ( 21 ) yields

$$({}^1\boldsymbol{R}_k\boldsymbol{c}_{k,i}+{}^1\boldsymbol{t}_k-\boldsymbol{r})(d\,{}^1\boldsymbol{R}_k\boldsymbol{c}_{k,i}+d\,{}^1\boldsymbol{t}_k-d\boldsymbol{r})=0 \qquad k=1,2,3 \qquad (22)$$

where $d^1\boldsymbol{R}_1 = d^1\boldsymbol{t}_1 = 0$. However, $d^1\boldsymbol{R}_k = {}^1\boldsymbol{R}_k{}^T\Omega({}^1\delta_k)$, where ${}^1\delta_k$ is the orientation error vector of ${}^1\boldsymbol{R}_k$ and $\Omega(\boldsymbol{v})$ denotes the skew symmetric matrix of vector $\boldsymbol{v}$. Notice also $\Omega({}^1\delta_k)\boldsymbol{c}_{k,i} = -\,\Omega(\boldsymbol{c}_{k,i})\,{}^1\delta_k$ . Therefore,

$$d^1\boldsymbol{R}_k\boldsymbol{c}_{k,i} = {}^1\boldsymbol{R}_k{}^T\Omega({}^1\delta_k)\boldsymbol{c}_{k,i} = -\,{}^1\boldsymbol{R}_k{}^T\Omega(\boldsymbol{c}_{k,i})\,{}^1\delta_k \qquad (23)$$

Substituting ( 23 ) into ( 22 ) yields

$$({}^1\boldsymbol{R}_k\boldsymbol{c}_{k,i}+{}^1\boldsymbol{t}_k-\boldsymbol{r})(-{}^1\boldsymbol{R}_k{}^T\Omega(\boldsymbol{c}_{k,i})\,{}^1\delta_k+d\,{}^1\boldsymbol{t}_k-d\boldsymbol{r})=0 \qquad k=1,2,3 \qquad (24)$$

The Jacobain matrix can be obtained by solving $d\boldsymbol{r}$ from ( 24 ). In this case, the (12×1) parameter vector $\rho_a$ consists of ${}^1\delta_2$ , ${}^1\delta_3$ , $\mathrm{d}^1\mathbf{t}_2$ and $d^1\boldsymbol{t}_3$. Let $\boldsymbol{v}_k \equiv {}^1\boldsymbol{R}_k\boldsymbol{c}_{k,i} + {}^1\boldsymbol{t}_k - \boldsymbol{r}$, $\boldsymbol{v}_k$ is the vector from the origin of the $k$th tracker frame to the target. Since ${}^1\boldsymbol{t}_1 = 0$, $d^1\boldsymbol{t}_1 = 0$, equation ( 24 ) can be written as

$$\boldsymbol{H}d\boldsymbol{r} = \begin{bmatrix} 0 & 0 \\ \boldsymbol{v}_2^T & 0 \\ 0 & \boldsymbol{v}_3^T \end{bmatrix} \begin{bmatrix} d\,{}^1\boldsymbol{t}_2 \\ d\,{}^1\boldsymbol{t}_3 \end{bmatrix} + \begin{bmatrix} 0 & 0 \\ \boldsymbol{v}_2^{T\,1}\boldsymbol{R}_2\Omega({}^1\boldsymbol{c}_{2,i}) & 0 \\ 0 & \boldsymbol{v}_3^{T\,1}\boldsymbol{R}_3\Omega({}^1\boldsymbol{c}_{3,i}) \end{bmatrix} \begin{bmatrix} {}^1\boldsymbol{\delta}_2 \\ {}^1\boldsymbol{\delta}_3 \end{bmatrix} \tag{25}$$

where

$$\boldsymbol{H} = \begin{bmatrix} \boldsymbol{v}_1^T \\ \boldsymbol{v}_2^T \\ \boldsymbol{v}_3^T \end{bmatrix} \tag{26}$$

***Theorem* 1:** The Jacobian of the multiple-beam system can be written into the following form,

$$\boldsymbol{J} = \boldsymbol{H}^{-1} \begin{bmatrix} 0 & 0 & 0 & 0 \\ \boldsymbol{v}_2^T & 0 & \boldsymbol{v}_2^{T\,1}\boldsymbol{R}_2\Omega({}^1\boldsymbol{c}_{2,i}) & 0 \\ 0 & \boldsymbol{v}_3^T & 0 & \boldsymbol{v}_2^{T\,1}\boldsymbol{R}_3\Omega({}^1\boldsymbol{c}_{3,i}) \end{bmatrix} \tag{27}$$

if and only if the three vectors connecting origins of the three tracker frames to the target point are linearly independent.

**Proof.** The necessary and sufficient condition for the matrix $\boldsymbol{H}$ to be invertible is that the three vectors $\boldsymbol{v}_k$ are independent. $\boldsymbol{v}_k$ represents the vector from the $k$th tracker to the target. Therefore, in order to write the Jacobian in the form ( 27 ), the three vectors from the origins of the three tracker frames to the target point should be independent.

Q.E.D.

Theorem 1 illustrates that one of the necessary conditions for the constrained system to be observable is that the three trackers do not lie on the same line. Otherwise, the three vectors from the three trackers to the target point are dependent.

The parameter error vector is observable if the Jacobian matrix of the error system is non-singular [12]. Examination of the Jacobian matrix structure, reveals the following fact:

***Theorem* 2:** The orientational error parameters of the $k$th tracker are not observable whenever the mirror center offset of the tracker is zero.

**Proof:** Whenever the mirror center offset of the $k$th tracker is zero, $\Omega(c_{k,i}) \equiv 0$. The corresponding terms in the Jacobian matrix are also zero. Consequently, the corresponding error parameters are not observable.

Q.E.D.

Theorem 2 reveals a serious problem. By using the error model ( 22 ), the algorithm is not robust due to the fact that the Jacobian matrix is near singularity all the time. This is because the mirror center offset of each tracker is very small. This fact prompted the authors to devise the following alternative scheme for the calibration of the multiple-beam system. The proof of Theorem 2 also shows that the orientation error of ${}^1\boldsymbol{T}_k$ is of secondary importance, compared to its positional error.

We can calibrate in advance the transformations ${}^1\boldsymbol{T}_2$ and ${}^1\boldsymbol{T}_3$ , assuming that each tracker can independently measure the target points. After ${}^1\boldsymbol{T}_2$ and ${}^1\boldsymbol{T}_3$ are determined, we then further improve the accuracy of ${}^1\boldsymbol{t}_2$ and ${}^1\boldsymbol{t}_3$ by using an iterative method. In this case, the error model is

$$({}^1\boldsymbol{R}_k \boldsymbol{c}_{k,i} + {}^1\boldsymbol{t}_k - \boldsymbol{r})(d\,{}^1\boldsymbol{t}_k - d\boldsymbol{r}) = 0 \qquad k = 1, 2, 3$$

with $d^1\boldsymbol{t}_1 = 0$. Again, Let $\boldsymbol{v}_k \equiv {}^1\boldsymbol{R}_k\boldsymbol{c}_{k,i} + {}^1\boldsymbol{t}_k - \boldsymbol{r}$, $\boldsymbol{v}_k$ is the vector from the $k$th tracker to the target. Let $\boldsymbol{H} = \begin{bmatrix} \boldsymbol{v}_1^T \\ \boldsymbol{v}_2^T \\ \boldsymbol{v}_3^T \end{bmatrix}$. Then the above becomes

$$\boldsymbol{H}d\boldsymbol{r} = \begin{bmatrix} 0 & 0 \\ \boldsymbol{v}_2^T & 0 \\ 0 & \boldsymbol{v}_3^T \end{bmatrix} \begin{bmatrix} d^1\boldsymbol{t}_2 \\ d^1\boldsymbol{t}_3 \end{bmatrix} \tag{28}$$

The corresponding Jacobian is

$$\boldsymbol{J} = \boldsymbol{H}^{-1} \begin{bmatrix} 0 & 0 \\ \boldsymbol{v}_2^T & 0 \\ 0 & \boldsymbol{v}_3^T \end{bmatrix}, \tag{29}$$

provided that $\boldsymbol{H}$ is invertible. The observability of $d^1\boldsymbol{t}_2$ and $d^1\boldsymbol{t}_3$ is further investigated next.

To estimate the unknown ${}^1\boldsymbol{t}_2$ and ${}^1\boldsymbol{t}_3$, at least three measurements must be taken. The corresponding Identification Jacobian is

$$\begin{bmatrix} \boldsymbol{H}_1^{-1} & 0 & 0 \\ 0 & \boldsymbol{H}_2^{-1} & 0 \\ 0 & 0 & \boldsymbol{H}_3^{-1} \end{bmatrix} \begin{bmatrix} 0 & 0 \\ \boldsymbol{v}_{2,1}^T & 0 \\ 0 & \boldsymbol{v}_{3,1}^T \\ 0 & 0 \\ \boldsymbol{v}_{2,2}^T & 0 \\ 0 & \boldsymbol{v}_{3,2}^T \\ 0 & 0 \\ \boldsymbol{v}_{2,3}^T & 0 \\ 0 & \boldsymbol{v}_{3,3}^T \end{bmatrix} \tag{30}$$

where the second index of $\boldsymbol{v}$ and the index of $\boldsymbol{H}$ denotes the first, second and third measurement.

***Theorem* 3:** Assume that three target points $\boldsymbol{r}_1$, $\boldsymbol{r}_2$, and $\boldsymbol{r}_3$ are measured. The vector from $k$th tracker to $j$th target point is $\boldsymbol{v}_{k,j}$. The Identification Jacobian of the multiple-beam laser tracking system is non-singular if and only if

(1) The three vectors $\boldsymbol{v}_{k,j}$ ($k$ = 1, 2, 3) are linearly independent when $j$ = 1, 2, 3, and,

(2) At least three independent target measurements are obtained by the second and third trackers.

The proof of Theorem 3 is given in the Appendix. The three independent target measurements obtained by the second tracker means that the vectors originating from the origin of the tracker frame to the three target points are independent, and the same for a suitable is third tracker. Note that in order to iteratively solve for the unknown parameter error vector, an initial condition must be given. Since ${}^1\boldsymbol{T}_2$ and ${}^1\boldsymbol{T}_3$ can be determined in a closed form with the assumption that the gimbal angular measurements are accurate, the initial condition is not difficult to obtain. Moreover, the result obtained in this section is essential for the study given in the next section.

### 3.2 Case 2: gimbal angular measurements are not sufficiently accurate

When angular measurements of the trackers are not sufficiently accurate, the unknowns are ${}^1\boldsymbol{T}_2$ and ${}^1\boldsymbol{T}_3$ as well as $\Delta l_k$ for each tracker. As discussed in Section 3.1, the rotation matrices ${}^1\boldsymbol{R}_2$ and ${}^1\boldsymbol{R}_3$ can be pre-calibrated in advance with the assumption that the uncertainty in the gimbal angular measurements is negligible. Furthermore as their accuracy is of secondly importance compared with that of the position vectors, the remaining task is to calibrate ${}^1\boldsymbol{t}_2$ and ${}^1\boldsymbol{t}_3$ and $\Delta l_k$ for $k = 1, 2, 3$.

The governing equations for computing target point $r$ using distance measurement are

$$({}^1\boldsymbol{R}_k \boldsymbol{c}_{k,i} + {}^1\boldsymbol{t}_k - \boldsymbol{r})^T({}^1\boldsymbol{R}_k \boldsymbol{c}_{k,i} + {}^1\boldsymbol{t}_k - \boldsymbol{r}) = (l_k^0 + \Delta l_k)^2 \qquad k = 1, 2, 3 \qquad (31)$$

where $c_{k,i}{}^0$ and $l_k{}^0$ are the predicted quantities before compensation. Perturbing both sides of the equation yields,

$$({}^1\boldsymbol{R}_k \boldsymbol{c}_{k,i} + {}^1\boldsymbol{t}_k - \boldsymbol{r})^T(d\,{}^1\boldsymbol{t}_k - d\boldsymbol{r}) = (l_k^0 + \Delta l_k) d\Delta l_k \quad k = 1, 2, 3 \qquad (32)$$

Since $l_k = l_k{}^0 + \Delta l_k$, thus

$$({}^{1}\boldsymbol{R}_k \boldsymbol{c}_{k,i} + {}^{1}\boldsymbol{t}_k - \boldsymbol{r})^T (d\,{}^{1}\boldsymbol{t}_k - d\boldsymbol{r}) = l_k d\Delta l_k \qquad (33)$$

Since $d^1\boldsymbol{t}_1 = 0$, equation ( 33 ) is equivalent to the set of equations

$$-\boldsymbol{v}_1^{\;T} \cdot d\mathbf{r} = l_1\, d\Delta l_1 \qquad (34)$$

$$\boldsymbol{v}_2^{\;T} (d^1\mathbf{t}_2 - d\mathbf{r}) = l_2 d\Delta l_2 \qquad (35)$$

$$\boldsymbol{v}_3^{\;T} (d^1\mathbf{t}_3 - d\mathbf{r}) = l_3 d\Delta l_3 \qquad (36)$$

Equations ( 34 ) – ( 36 ) can be rewritten in the following matrix form,

$$\mathbf{H} d\mathbf{r} = \begin{bmatrix} 0 & 0 \\ \mathbf{v}_2^T & 0 \\ 0 & \mathbf{v}_3^T \end{bmatrix} \begin{bmatrix} d^1\mathbf{t}_2 \\ d^1\mathbf{t}_3 \end{bmatrix} + \begin{bmatrix} l_1 & 0 & 0 \\ 0 & l_2 & 0 \\ 0 & 0 & l_3 \end{bmatrix} \begin{bmatrix} d\Delta l_1 \\ d\Delta l_2 \\ d\Delta l_3 \end{bmatrix} \qquad (37)$$

According to Theorem 1 $\boldsymbol{H}$ can be moved to the right-hand side of ( 36 ) if the three vectors from the three trackers to the target point are independent. In this case, the corresponding Jacobian is

$$\boldsymbol{J} = \boldsymbol{H}^{-1} \begin{bmatrix} 0 & 0 & l_1 & 0 & 0 \\ \boldsymbol{v}_2^T & 0 & 0 & l_2 & 0 \\ 0 & \boldsymbol{v}_3^T & 0 & 0 & l_3 \end{bmatrix} \qquad (38)$$

I order to estimate the unknowns, at least 4 measurements have to be taken. The Identification Jacobian of the system is obtained by stacking multiple Jacobians $\boldsymbol{J}$ of the form ( 38 ).

***Theorem* 4:** Assume that four measurements are taken. The Identification Jacobian of the multiple-beam laser tracking system is singular if and only if

$$\boldsymbol{u}_{k,4} = a_k \boldsymbol{u}_{k,1} + b_k \boldsymbol{u}_{k,2} + c_k \boldsymbol{u}_{k,3} \qquad (39)$$

where $a_k$, $b_k$, $c_k$ are scalars satisfying

$$a_k + b_k + c_k = 1$$

and $\boldsymbol{u}_{kj} = \boldsymbol{v}_{kj} / \| \boldsymbol{v}_{kj} \|$ for $k = 1, 2$ and $j = 1, 2, 3, 4$. The proof of Theorem 4 is given in the Appendix. The physical meaning can be explained from studying the matrix given in (46). It can be rewritten as $\begin{bmatrix} \boldsymbol{u}_{k,1}^T & 1 \\ \boldsymbol{u}_{k,2}^T - \boldsymbol{u}_{k,1}^T & 0 \\ \boldsymbol{u}_{k,3}^T - \boldsymbol{u}_{k,1}^T & 0 \\ \boldsymbol{u}_{k,4}^T - \boldsymbol{u}_{k,1}^T & 0 \end{bmatrix}$. Then necessary and sufficient condition for the matrix to be nonsingular is that the last three elements of the first column $\boldsymbol{u}_{k,2} - \boldsymbol{u}_{k,1}$, $\boldsymbol{u}_{k,3} - \boldsymbol{u}_{k,1}$, $\boldsymbol{u}_{k,4} - \boldsymbol{u}_{k,1}$ are linearly independent. This implies that using a single-plane constraint, one cannot calibrate a multiple-tracker system, since the three vectors will always be singular in this case.

## 4 Simulation and Experimental Results

One of the objectives of the simulation study is to verify whether the three-plane three-tracker setup works at all and can be applied to calibrate a multi-beam LTS. Another objective is to compare calibration results between the method that uses both the angular and distance measurements and the one that uses only distance measurements. In the case of using angular measurements, it is assumed that these measurements are much less accurate than the distance measurements. Under this assumption we need to see if the coarse angular measurements can improve the calibration performance, as the theory predicts. Experimental verification data was collected using the LTS in the Robotic Center at Florida Atlantic University. The data was used to calibrate the multi-beam LTS model.

### 4.1 Simulation results

The simulation program models three laser trackers and three calibration planes. Refer to Figure 6 for the system setup. The actual values of the parameters of the trackers and the planes are listed in

Table 1 and Table 2. The values of the parameters dictating the transformation matrices relating the coordinate systems of trackers III and I, trackers II and I are presented in Table 3. The planes are placed so that their normals are linearly independent. Noise is added to the angular and distance measurements. Likewise the noise added to the angular measurements is uniformly distributed between -30 μrad and 30 μrad. The noise added to the distance measurements is [-1μm 1μm]. A noise uniformly ranging from -10μm to 10μm is added to the 3D measurements to simulate the situation that the plane may not be perfectly smooth.

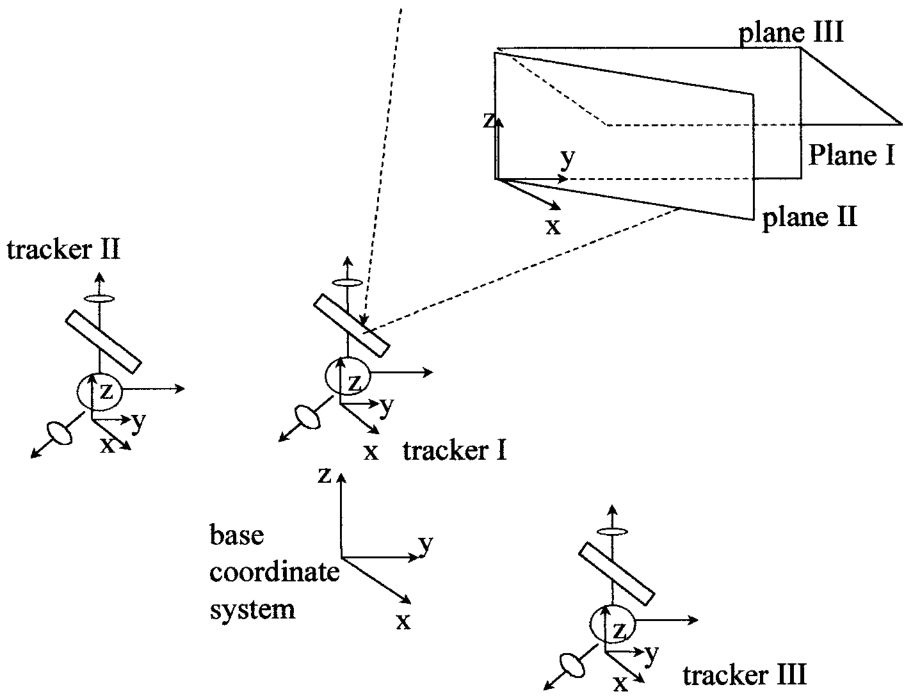


Figure 6 System setup of the calibration of a multiple-beam LTS

Table 1 Plane parameters under system setup II

| Parameters | Plane I | Plane II | Plane III |
|---|---|---|---|
| $\boldsymbol{n}$ | {-1, 0, 0} | {-cos(10°), -sin(10°), 0} | {-cos(10°), 0, -sin(10°)} |
| $a$(m) | 1 | cos(10°) | cos(10°) |

Table 2 The actual values of the parameters of the three trackers

| Parameters | tracker I | Tracker II | tracker III |
|---|---|---|---|
| $^{*}\boldsymbol{b}_I$ | {-0.5012, -0.8661, 0.0013} | {-0.5012, -0.8661, 0.0013} | {-0.5012, -0.8661, 0.0013} |
| $l_r$ (mm) | 2000.1 | 2000.1 | 2000.1 |
| $\{c_x, c_y\}$(mm) | { 0.1, 0.1 } | { 0.1, 0.1 } | { 0.1, 0.1 } |
| $\{a_1, e_2\}$ (mm) | { 0.01, 0.01 } | { 0.01, 0.01 } | { 0.01, 0.01 } |
| $\{\alpha_1, d\theta_2, \alpha_2\}$ | {90.1°, 90.1°, 90.02°} | {90.1°, 90.1°, 90.02°} | {90.1°, 90.1°, 90.02°} |

Table 3 The parameters in the transformation matrix between coordinate systems of the laser trackers

| Parameters in the transformation matrix | From tracker II to I | from tracker III to I |
|---|---|---|
| $\delta_x$ (degree) | 0 | 0 |
| $\delta_y$ (degree) | -10° | -10° |
| $\delta_z$ (degree) | 10° | -10° |
| $x$ (m) | -0.35 | 0.35 |
| $y$ (m) | 0 | 0 |
| $z$ (m) | -0.5 | -0.5 |

The calibration procedures are outlined in [10]. The three trackers are calibrated individually using a nonlinear least-squares procedures. As a result, all the parameters of each tracker are obtained. The parameters of the transformation matrices relating different trackers are also estimated. Then the 6 translational parameters and 3 beam distance offsets are fine tuned using the measurements from all the three trackers. Figure 7 and Figure 8 show the simulation results for both calibrations. The $y$ axes of both figures represent the maximum, mean and minimum values of the difference between the computed target coordinates and the actual target coordinates. The $x$ axis represents the number of measurements used in the simulation. The condition numbers for both calibrations are between $10^3$ and $10^4$. It is obvious that the target coordinate error from the calibration using both angular and distance measurements is by order of magnitude smaller than that from the calibration using distance measurements only. This demonstrates that the angular measurements can still be successfully used to compute the mirror center offset.

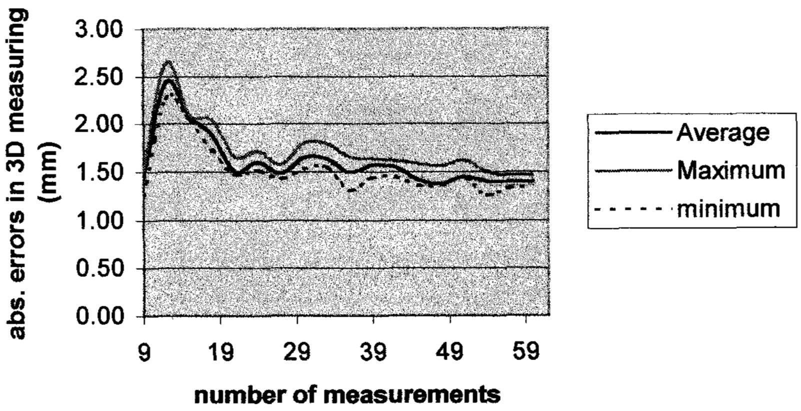


Figure 7 The calibration of the multiple-beam laser tracking system using distance measurements only

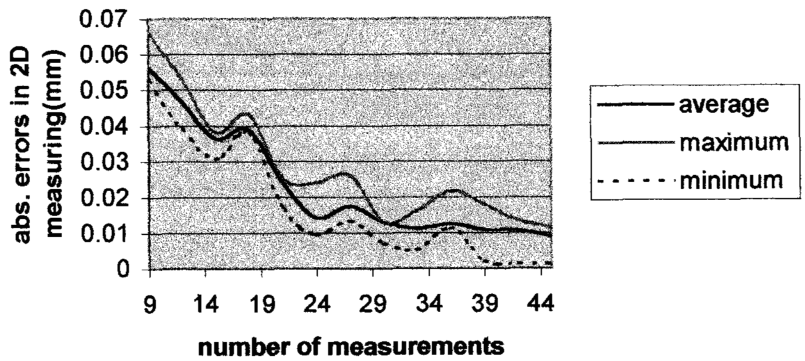


Figure 8 The calibration of multiple-beam laser tracking system using both angular and distance measurements

## 4.2 Experimental results

### 4.2.1 Experiment setup

An experiment multi-beam laser tracking system was built and tested at the FAU Robotics Lab (see Figure 9 ). Figure 10 shows the manual driven Mitutoyo CX-D2 coordinate measuring machine (CMM) used to emulate the calibration planes. Each tracking unit uses an HP 10705A laser interferometer system and several HP 10701A beam splitters to direct the laser beam towards to the tracking mirror. The tracking mirror is mounted on a Aerotech rotary table. A corner-cube retroreflector is firmly mounted on the CMM which was located at a distance of 2m away from the gimbals. The CMM has a nominal accuracy of 0.05mm, a repeatability of 0.01mm and a work volume of $400\times500\times800mm^3$. The window of the tracking mirror is 19mm in diameter while the cross-section diameter of the laser beam is approximately 8mm in diameter. To implement each tracker gimbal, an Aerotech ADR150-2 direct-drive rotary stage is installed for the vertical axis, and Aerotech ADR200-5 direct-drive rotary stage is used for the horizontal axis. The angular encoder accuracy of both rotary tables is around 5 arcseconds.

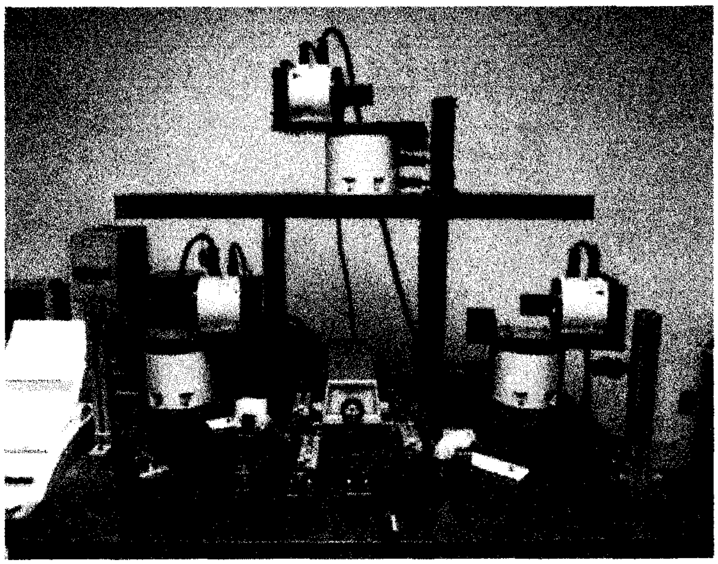

Figure 9 The Experiment Setup of the Multiple-beam Laser Tracking System

Figure 11 illustrates schematically the relative locations of the three trackers and the CMM. The coordinates marked on each tracker were measured by plain rulers. These are respect to the CMM coordinate system. Two of the trackers are placed in the front row and are approximately 0.70m apart. The third tracker is placed about 0.50m higher than the two trackers. Two sets of experimental data were collected. The second set of data was collected on a different day from the first one. For the first set of experimental data, the CMM was used to form three planes by being placed in three different orientations and places. In the first place, the CMM was manually driven to move along $x$ and $y$ axes so that these points are on the same plane. Thirty points were measured on the first plane. Then the rotary table on which the CMM was situated rotated a certain degree about its vertical axis. Again the CMM was manually driven to move along $x$ and $y$ axes to so that 30 points were measured. In this way, the 30 points were on a second plane. Similarly for the third plane. Similar procedures were applied to obtain the second set of experimental data. This time, the rotary table on which the CMM was situated was moved approximately 0.3m closer to the trackers. Then the CMM was manually rotated twice to form three planes. On each plane, 20 points were measured. The following calibration used the first set of experimental data to calibrate the parameters of the laser trackers and the planes. The second set of experimental data were used for verification.

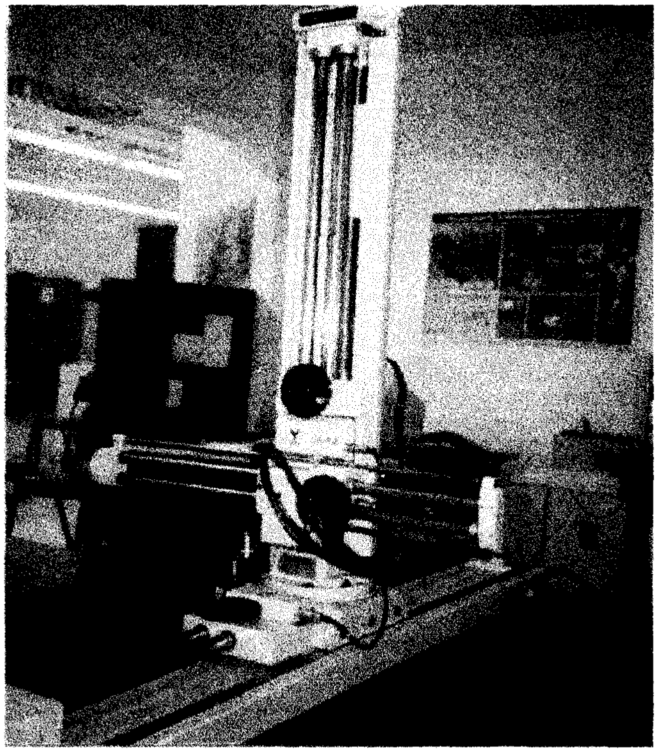

Figure 10 Mitutoyo CX-D2 Coordinate Measuring Machine in the Robotics Center at FAU

In addition to the experiments described above, a third set of experimental data was collected from a similar experimental setup one year before. In that experiment, a glass plane instead of a CMM was used to construct the calibration planes. Similarly, the glass plane was situated on a rotary table. During the experiments, the glass plane was placed at 3 different orientations and positions to form three planes. In the first position, 23 points on the glass plane were measured by the three trackers. Two more subsets of data were collected after the glass plane was placed with different positions and orientations. The calibration model was applied to this third set of measured data more than a year after it was taken.

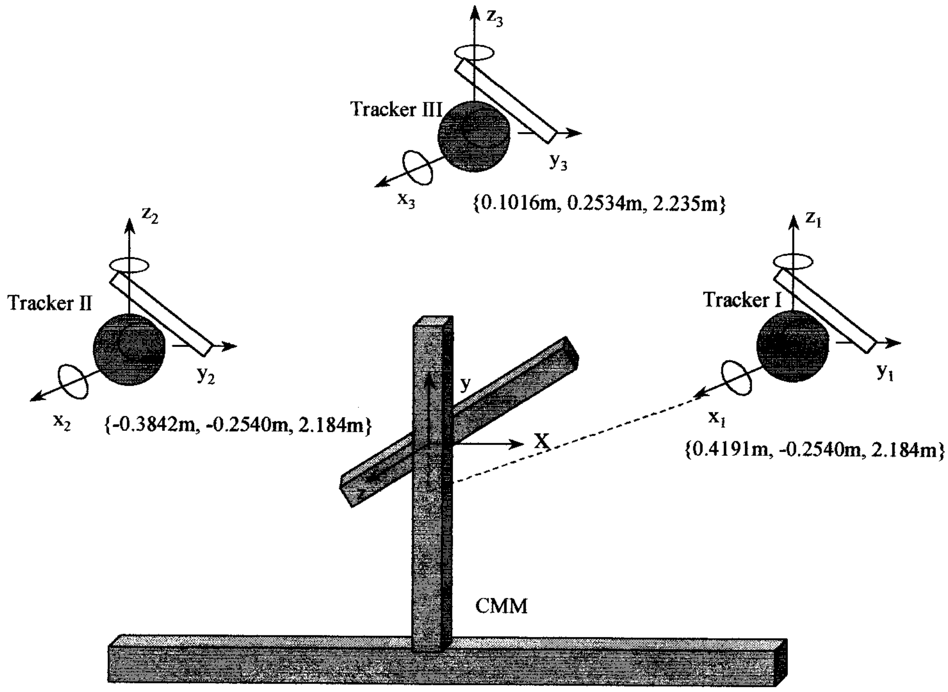


Figure 11 The geometric setup of the multiple-beam laser tracker and CMM

### 4.2.2 Experimental results

The calibration of the multiple-beam LTS consists of two stages. The first stage involves the calibration of the individual laser trackers. The second stage is for calibrating the 6 positional parameters and for fine tuning the 3 beam length offset. The 10-parameter model and multiple plane constraint are used in the calibration. The procedures shown in [6,10] can be used to calibrate the parameters of each tracker first. The parameters of the mirror center offset and gimbal axis misalignment are constrained by (40). The reason for constraining the parameters is that these parameters sometimes tend to reach unrealistic values after the calibration. Constraining them within a practical range is a way to ensure that the error does not propagate much. In the first set of experimental data, 30 points were measured on each plane. Twenty-five points are used in the calibration and the remaining 5 points are used in the verification. The calibrated parameters are shown in Table 4.

$$-2\text{mm} < \boldsymbol{c}_x, \boldsymbol{c}_y < 2\text{mm}, \qquad -1\text{mm} < \boldsymbol{e}_2 < 1\text{mm}, \qquad -1\text{mm} < \boldsymbol{a}_1 < 1\text{mm} \tag{40}$$

In the second stage, the parameters to be calibrated in the multiple-beam laser tracking system are the three beam length offset and the translation vectors relating the coordinate system of tracker II to tracker I and tracker III to tracker I. A standard pose algorithm [13] can be used to estimate the rotation matrices and the translation vectors based on all the parameters in the system and the measurements. These can be used as the initial guess of the parameters to be calibrated. The initial values for the beam length offset can be set as those in Table 4. The procedures for the calibration of multiple-beam laser tracker using both angular and distance measurements are used in the calibration.

Figure 11 shows the calibration results. The horizontal axis represents the number of measurements used in the calibration and the vertical axis denotes the values of the plane residue. The plane residual is given in maximum, average and minimum values. The algorithm converged after 5 iterations. The condition number is in the order of magnitude of $10^5$. The average plane residual reaches 0.04mm at the end of iterations. The parameters calibrated from using the first set of experimental data can also be verified against the second set of experimental data. The calibrated parameters are used along the angular and distance measurements of the second experimental data to compute the 3-D coordinates. The plane residual is about 0.4mm which is 10 times worse than that of the calibration.

Table 4 The values of the calibrated parameters of tracker I and II and III (part I)

| | tracker I | tracker II | tracker III |
|---|---|---|---|
| $l_r$ (m) | 1.5401 | 1.4788 | 1.6744 |
| $\boldsymbol{b_I}$ | [0.9890 0.0340 0.1442] | [-0.9824 0.1408 0.1229] | [0.9049 0.4114 0.1095] |
| $[c_x, c_y]$ (m) | [-0.0017 0.0010] | [0.0014 -0.0010] | [0.0013 0.0010] |
| $d\theta_2$ (radian) | 1.5708 | 1.5714 | 1.5719 |
| $\alpha_1$ (radian) | 1.5712 | 1.5719 | 1.5718 |
| $\alpha_2$ (radian) | 1.5716 | 1.5717 | 1.5719 |
| $e_2$ (m) | 0.0013 | 0.0010 | 0.0015 |
| $a_1$ (m) | 0.0014 | 0.0010 | 0.0013 |
| $n_1$ | [0.9586 0.2794 -0.0555] | [0.9072 -0.1257 0.4016] | [0.8611 -0.4059 0.3061] |
| $a_1$ (m) | 2.1089 | 1.7885 | 2.2396 |
| $n_2$ | [0.9564 0.2287 -0.1817] | [0.9697 -0.1253 0.2098] | [0.8951 -0.3191 0.3114] |
| $a_2$ (m) | 2.0276 | 2.0358 | 2.1339 |
| $n_3$ | [0.9777 0.2078 -0.0296] | [0.9347 0.0523 0.3516] | [0.7962 -0.5339 0.2847] |
| $a_3$ (m) | 2.1595 | 1.8230 | 2.2521 |

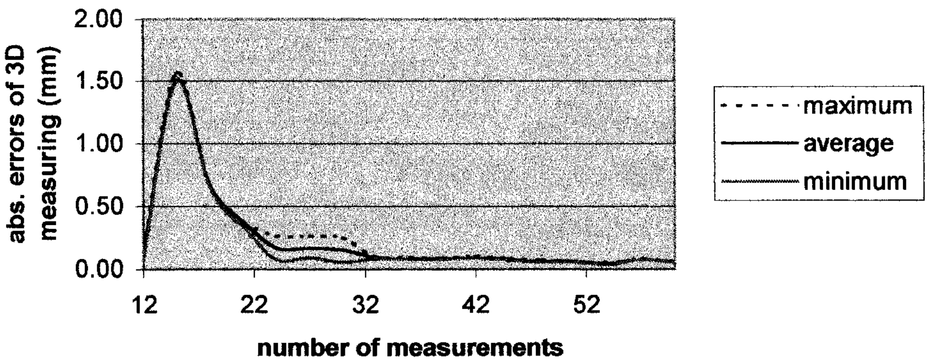


Figure 11 Calibration results of the multiple tracker and multiple plane using the first set of experimental data

Similar calibration procedures can be executed to calibrate the three trackers using the third set of experimental data. This time 15 out of 23 measured points on each plane were used in the identification experiment, and the rest 8 points were used in the verification experiment. The calibrated parameters are listed in Table 5. The condition number is in the order of $10^5$. Figure 12 shows the calibration results. The average plane residual reached 15μm at the end of the iterations. This is definitely better than the result of the calibration using the first set of experimental data. One reason for the smaller plane residuals is that the smoothness of the glass plane is better than that of the planes formed by CMM. Another reason is that the third set of experimental data was collected within a smaller workspace than the first one.

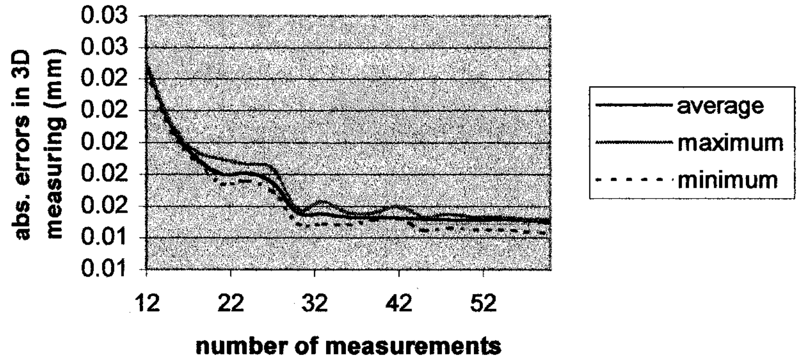


Figure 12 Calibration results of the multiple tracker and multiple plane using the third set of experimental data

Table 5 The values of the calibrated parameters of tracker I and II and III (Part II)

| | tracker I | tracker II | tracker III |
|---|---|---|---|
| $l_r$ (m) | 0.8826 | 0.7692 | 0.7467 |
| $\boldsymbol{b_I}$ | [0.0154 0.9776 -0.2098] | [ -0.0121 0.9952 -0.0970] | [0.0936 0.4254 -0.9002] |
| $[c_x, c_y]$ (m) | [-0.0014 0.0011] | [0.0017 -0.0008] | [0.0010 0.0014] |
| $d\theta_2$ (radians) | 1.5703 | 1.5717 | 1.5716 |
| $\alpha_1$ (radians) | 1.5714 | 1.5717 | 1.5716 |
| $\alpha_2$ (radians) | 1.5713 | 1.5716 | 1.5718 |
| $e_2$ (m) | 0.0010 | 0.0011 | 0.0011 |
| $a_1$ (m) | 0.0012 | 0.0011 | 0.0014 |
| $\boldsymbol{n}_1$ | [-0.0659 0.2117 0.9751] | [-0.0716 0.0966 0.9927] | [0.0532 -0.9058 -0.4203] |
| $a_1$ (m) | 0.0894 | 0.0411 | 0.0042 |
| $\boldsymbol{n}_2$ | [-0.0943 0.2108 0.9730] | [-0.0905 0.0959 0.9913] | [-0.0007 -0.9055 -0.4244] |
| $a_2$ (m) | 0.0894 | 0.0411 | 0.0040 |
| $\boldsymbol{n}_3$ | [-0.0659 0.2117 0.9751] | [-0.0716 0.0966 0.9927] | [0.0532 -0.9058 -0.4203] |
| $a_3$ (m) | 0.0894 | 0.0411 | 0.0042 |

## 5 Summary

In this paper, a methodology for self-calibration of a laser tracking measurement system is proposed. Kinematic models that describe not only the motion but also geometric variations of system are developed. Various calibration strategies utilizing planar constraints are proposed to deal with different system setups. For each calibration strategy, issues about the error parameter estimation of the system are explored to find out under which conditions these parameters can be uniquely estimated. These conditions reveal the applicability of the planar constraints to the system self-calibration. Through error analysis, it is found that the angular measurement may still be used to predict the coordinates of the beam incidence at the mirror surface of the each tracker, even though the angular measurement of a gimbal is inferior to the distance measurement in a laser. This claim is also backed by the simulation studies. The simulation and experimental studies also support the claim that the three-plane three-tracker setup can be applied to calibrate the multi-beam LTS.

### *Reference*


[1] Lau, K., Hocken, R., Haight W., "Automatic Laser Tracking Interferometer System for Robot Metrology," *Precision Engineering*, Vol. 8, No.1, pp3-8, 1986.

[2] Lau, K., Hocken, R., Haynes, L., "Robot Performance Measurements Using Automatic Laser Tracking Techniques," *Robotics & Computer-Integrated Manufacturing*, Vol.2, No. ¾, pp.227-236, 1985.

[3] Chesapeake Laser Systems, INC., "The CMS-2000 Laser Coordinate Measuring System", 1994.

[4] Zhuang, H., Li, B., Roth, Z.S., Xie, X., "Self-calibration and Mirror Center Offset Elimination of a Multi-beam Laser Tracking System," *Robotics and Autonomous Systems,* Vol.9, pp. 255-269, 1992.

[5] Zhuang, H., "Kinematic Modeling, Identification and Compensation of Robot Manipulator," Ph.D. Dissertation, Florida Atlantic University, 1989.

[6] Zhuang, H., Roth, Z.S., "Modeling Gimbal Axis Misalignment and Mirror Center Offset in a Single-beam Laser Tracking Measurement System," *The International Journal of Robotics Research*, Vol.14, 211-224, (1995).

[7] Mooring, B.W., "Calibration of A Laser Projection System," ASME, DSC-Vol. 29, pp 33-41, 1991.

[8] Payne, J.M., Parker, D., and Bradley, R.F., "Rangefinder with Fast Multipe Range Capability," *Review of Science Instrumentation*, Vol.63, No. 6, pp 3311-3316, 1992.

[9] Mayer, J.R., Parker, G., "A Protable Instrument for 3-D Dynamic Robot Measurements Using Triangulation and Laser Tracking", *IEEE Transactions on Robotics and Automation*, Vol. 10, No. 4, August, 1994, pp 504-515.

[10] Motaghedi, S. H., *Self-calibration of Laser Tracking Measurement System with Planar Constraints*, Ph.D. Dissertation, Florida Atlantic University, Boca Raton, FL, 1999.

[11] Zhuang, H., Motaghedi, S.H., Roth, Z.V., Bai, Y., "Robot Calibration with Planar Constraints", to appear on *IEEE International Conference on Robotics and Automation*, Detroit, May 1999.

[12] Everett L.J., Driels M., and Mooring B.W., "Kinematic Modeling for Robot Calibration", *Proceedings – 1987 IEEE International Conference on Robotics and Automation*, pp 792-797, Philadelphia, April, 1987.

[13] Zhuang, H. and R. Sudhakar, "Simultaneous rotation and translation fitting of two sets of 3D points," *IEEE Trans. Systems, Man, Cybernetics*, Vol. 27, No. 1, Feb. 1997, pp. 118-126.

## Appendix

**Proof of *Theorem 3.*** ( 30 ) is the Jacobian of the multiple-beam laser tracking system.

$\begin{bmatrix} \boldsymbol{H}_1^{-1} & 0 & 0 \\ 0 & \boldsymbol{H}_2^{-1} & 0 \\ 0 & 0 & \boldsymbol{H}_3^{-1} \end{bmatrix}$ is non-singular if $\boldsymbol{H}_j$ ( $j$ = 1, 2, 3 ) is non-singluar. . According to *Theorem 1*, $\boldsymbol{H}_j$ ( $j$ = 1, 2, 3 ) is non-singular if and only if $v_{k,j}$.($i$=1,2, 3) are linearly independent.

Whenever at least three independent target measurements are obtained by the second and third trackers, the matrix made up of $v_{k,j}$ is non-singular, which is shown below. $\begin{bmatrix} 0 & 0 \\ \boldsymbol{v}_{2,1}^T & 0 \\ 0 & \boldsymbol{v}_{3,1}^T \\ 0 & 0 \\ \boldsymbol{v}_{2,2}^T & 0 \\ 0 & \boldsymbol{v}_{3,2}^T \\ 0 & 0 \\ \boldsymbol{v}_{2,3}^T & 0 \\ 0 & \boldsymbol{v}_{3,3}^T \end{bmatrix}$ can take the following form after rearranging its rows,

$$\begin{bmatrix} \boldsymbol{v}_{2,1}^T & 0 \\ \boldsymbol{v}_{2,2}^T & 0 \\ \boldsymbol{v}_{2,3}^T & 0 \\ 0 & \boldsymbol{v}_{3,1}^T \\ 0 & \boldsymbol{v}_{3,2}^T \\ 0 & \boldsymbol{v}_{3,3}^T \\ 0 & 0 \\ 0 & 0 \\ 0 & 0 \end{bmatrix} \tag{41}$$

( 41 ) is non-singular if and only if the two sub-matrices $\begin{bmatrix} \boldsymbol{v}_{2,1}^T \\ \boldsymbol{v}_{2,2}^T \\ \boldsymbol{v}_{2,3}^T \end{bmatrix}$ and $\begin{bmatrix} \boldsymbol{v}_{3,1}^T \\ \boldsymbol{v}_{3,2}^T \\ \boldsymbol{v}_{3,3}^T \end{bmatrix}$ are both non-singular. These two matrices are non-singular if and only if three target measurements obtained by the second and third trackers are independent.

**Proof of *Theorem 4.*** The condition of the matrix made up of $\boldsymbol{v}_{k,j}$ and $l_{k,j}$ being singular is the sub-matrix

$$\begin{bmatrix} \boldsymbol{v}_{k,1}^T & l_{k,1} \\ \boldsymbol{v}_{k,2}^T & l_{k,2} \\ \boldsymbol{v}_{k,3}^T & l_{k,3} \\ \boldsymbol{v}_{k,4}^T & l_{k,4} \end{bmatrix} \tag{42}$$

being singular, which is in return equivalent to the following matrix being singular

$$\begin{bmatrix} \boldsymbol{u}_{k,1}^T & 1 \\ \boldsymbol{u}_{k,2}^T & 1 \\ \boldsymbol{u}_{k,3}^T & 1 \\ \boldsymbol{u}_{k,4}^T & 1 \end{bmatrix} \tag{43}$$

Since $l_{k,j}$ = || $\boldsymbol{v}_{k,j}$||. Let $\alpha_k$, $\beta_k$, $\gamma_k$ and $\eta_k$ be scalars. If vectors $[\boldsymbol{u}_{k,j}^T \;\; 1]^T$ is not linearly independent, there exists a nonzero scalar, such that the following two equations are simultaneously satisfied,

$$\alpha_k \boldsymbol{u}_{k,1} + \beta_k \boldsymbol{u}_{k,2} + \gamma_k \boldsymbol{u}_{k,3} + \eta_k \boldsymbol{u}_{k,4} = 0 \tag{44}$$

where

$$\alpha_k + \beta_k + \gamma_k + \eta_k = 0 \tag{45}$$

Without the loss of generality, let us assume that $\eta_k$ is non-zero. From ( 44 ),

$$\boldsymbol{u}_{k,4} = a_k \boldsymbol{u}_{k,1} + b_k \boldsymbol{u}_{k,2} + c_k \boldsymbol{u}_{k,3} \tag{46}$$

where

$$a_k = -\alpha_k / \eta_k, \;\; b_k = -\beta_k / \eta_k, \;\; and \;\; c_k = -\gamma_k / \eta_k, \tag{47}$$

Substituting ( 45 ) into ( 46 ), it follows that

$$a_k = \alpha_k / (\alpha_k + \beta_k + \gamma_k), \;\; b_k = -\beta_k / (\alpha_k + \beta_k + \gamma_k), \;\; and \;\; c_k = -\gamma_k / (\alpha_k + \beta_k + \gamma_k)$$

( 48 )

Thus $a_k$ , $b_k$ , $c_k$ satisfy $a_k + b_k + c_k = 1$. On the other hand, if ( 39 ) and ( 45 ) do not hold simultaneously, there is not a nonzero $\eta_k$ , such that ( 44 ) and ( 45 ) are simultaneously satisfied. Consequently $[\boldsymbol{u}_{kj}^T \;\; 1]^T$ is linearly independent.